

Lysozyme Crystal Growth Kinetics Monitored Using a Mach–Zehnder Interferometer

E. H. SNELL,^{a†} J. R. HELLIWELL,^a T. J. BOGGON,^a P. LAUTENSCHLAGER^b AND L. POTTHAST^b

^aChemistry Department, University of Manchester, Oxford Road, Manchester M13 9PL, and ^bDornier GmbH, Raumfahrt-Infrastruktur, 88039 Friedrichshafen, Germany. E-mail: hell@man.ac.uk

(Received 14 June 1995; accepted 8 January 1996)

Abstract

A Mach–Zehnder interferometer has been developed for the monitoring of the kinetics of the diffusion process in protein crystal growth. This device can be used in conjunction with the ESA Advanced Protein Crystallization Facility (APCF), which allows experiments under microgravity conditions (*e.g.* on board the NASA Space Shuttle). Experimental trials on the ground have been carried out with the interferometer using the engineering model of the APCF and a protein dialysis reactor. Chicken egg-white lysozyme crystal growth, as a test, has thereby been monitored directly. The changes of concentration in the solution over time have been determined *via* the refractive index measurements made and subsequently correlated with visual monitoring of crystal growth in a repeat experiment.

1. Introduction

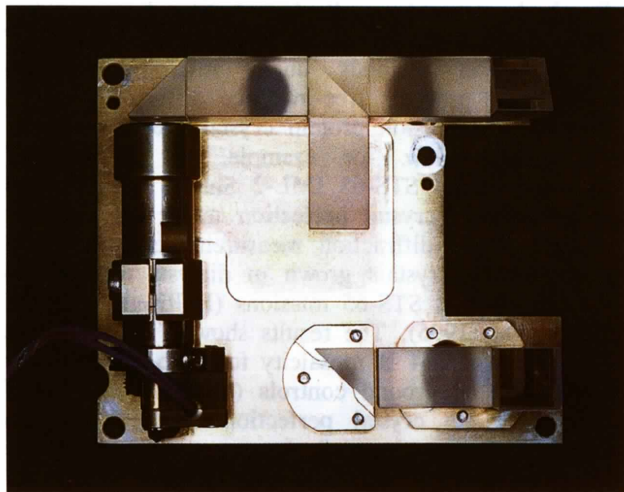
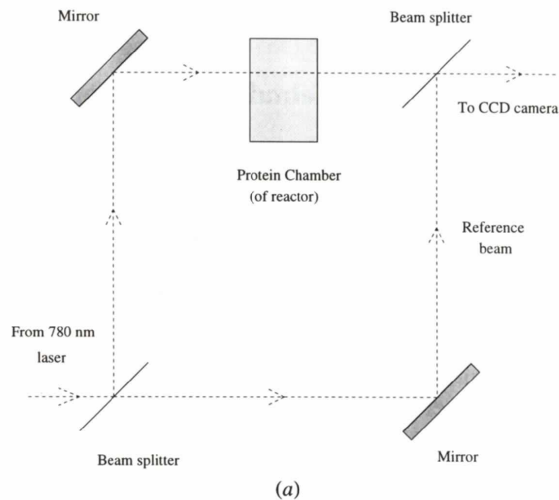
For the detailed understanding of protein crystal growth as a process it is necessary to perform diagnostic and monitoring experiments. Following the nucleation stage it is possible to consider monitoring, as a function of time, the changes in concentration in a solution of a precipitant agent and a protein by use of interferometry. Hence, a quantitative representation of the process of diffusion of protein and salt in a crystal growth chamber can be obtained. Such information should be useful to quantify the effect of differing chemical agents as well as physical parameters (*e.g.* temperature, gravity) on the crystal growth process in terms of fluid flow.

Different types of interferometer can be considered for the study of the refractive index changes to be expected in a protein crystal growth solution (Shlichta, 1986). These are notably the Michelson interferometer and the Mach–Zehnder interferometer designs. The advantage of the latter type is its compactness making it particularly suitable for

incorporation into existing apparatus used for microgravity experimentation *e.g.* the ESA Advanced Protein Crystallization Facility (APCF) developed for and now flown frequently on board NASA's Space Shuttle.

The APCF (Snyder, Fuhrmann & Walter, 1991; Bosch, Lautenschlager, Potthast & Stapelmann, 1992) was constructed to provide a wider range of crystallization methods under microgravity than hitherto. It provides free-interface diffusion, dialysis and vapour-diffusion protein crystal growth reactors. The APCF flew, for example, on the STS-57 Spacehab-1 and STS-65 IML-2 Shuttle missions. To assess protein crystal perfection under microgravity growth, X-ray diffraction measurements were made on lysozyme crystals grown in dialysis reactors on the STS-57 and STS-65 missions (Helliwell, Snell & Weisgerber, 1995). The results showed improvements of a factor of 3–4 in mosaicity for each mission over the associated ground controls (Snell *et al.*, 1995). Differences in crystal perfection between the two missions were observed however and raise the question of what is the actual optimum length of time, under microgravity conditions, for crystal growth to yield the best crystal quality. Moreover, even in the shorter mission (5 d), which yielded the best degree of perfection, there was still some imperfection manifest when comparing the measured mosaicity *versus* the theoretical limit (Snell *et al.*, 1995; Helliwell, 1988). Hence, interferometry diagnostic monitoring through a microgravity mission offers the prospect of restricting crystal growth to a period shorter than a mission duration *i.e.* so as to optimize the perfection of crystals. In the development of a Mach–Zehnder interferometer for the APCF it is essential to first undertake trials with it on the ground. Lysozyme was chosen as a test sample because our perfection measurements and calculations have been made with this system. Also, much is already known about it and it can be easily crystallized. This paper describes ground crystallization trials and studies with lysozyme using the engineering model of the APCF fitted with the Mach–Zehnder interferometer and the results it has produced.

† Current address: NASA Laboratory for Structural Biology, Code ES76, Building 4464, Marshall Space Flight Center, Huntsville, AL 35812, USA.



(b)

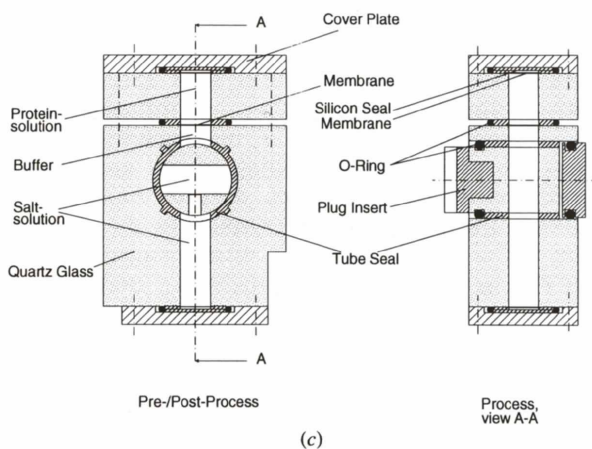


Fig. 1. (a) Schematic diagram of the Mach-Zehnder interferometer. (b) Photograph showing the interferometer with light path, laser, beam splitters and mirrors visible. (c) Schematic diagram of the dialysis crystallization reactor.

Table 1. Solutions filling the dialysis reactor

Reactor part	Filling solution
Protein chamber (188 μ l)	15.8 mg lysozyme (3 \times crystallized, dialyzed and lyophilized powder of chicken egg-white lysozyme) dissolved in 188 μ l 0.04 M acetate buffer (pH 4.7)
Buffer chamber (59 μ l)	0.04 M acetate buffer (pH 4.7)
Salt piston and reservoir (541 μ l)	7.34 g NaCl per 100 ml H ₂ O

2. Experimental

2.1. Instrument principles of operation

The Mach-Zehnder interferometer consists of two beam splitters and two totally reflecting mirrors. A schematic is shown in Fig. 1(a) with a photograph of the base plate in Fig. 1(b). The two light beams travel within the apparatus along separate paths. In one path the reactor is inserted such that the measurement beam passes through the protein chamber, and the resulting interference with the reference beam produces fringes. As the diffusion process carries on there is a change in the concentration of the solution in the reactor and a corresponding change in the refractive index. Consequently there is motion of fringes as crystallization takes place.

2.2. Crystallization reactor and conditions

The dialysis reactor used for crystallization in the APCF, shown as a schematic in Fig. 1(c), consists of two quartz glass blocks with one square-shaped volume for the protein solution and one for the salt solution and a small volume for buffer solution. The salt and small buffer volume are separated by a rotatable plug with a 'T'-shaped channel containing salt solution. The volumes are sealed with silicon rubber O rings and vacuum grease. In each volume there is a small air gap between the solutions and the chamber covers created by a special silicon seal and dialysis membrane to provide compensation for volume changes (*e.g.* due to slight variations in temperature). The protein chamber has plane surfaces permitting distortion-free optical observation. Metal inserts allow fixation of the cover plates and rotation of the plug. During the preprocess and postprocess phases the salt and protein chambers are separated. To start the process the plug is rotated by 90° so that all volumes come into contact and diffusion starts. At the end of the experiment the plug is again rotated by 90° to separate the chambers.

The lysozyme crystallization recipe used here was the same as for our STS-65 mission conditions, Table 1 (Snell *et al.*, 1995). In accord with the previous microgravity experiment (for which no interferometric monitoring was available) the protein chamber had been treated with a siliconization solution (Sigmacote) for a

period of 10 min. The reactor was filled and then kept at a constant temperature of 293 ± 0.1 K before and during crystallization.

2.3. Fringe pattern recording through the protein crystal growth process

The reactor was inserted into the engineering model of the APCF and a reference image was taken with no diffusion present (*i.e.* before the different solutions were allowed into contact with each other). The Mach-Zehnder interferometer is adjusted such that a minimum number of fringes, ideally none but experimentally one or two, are seen initially. The reference image recorded allows these to be taken into account. The reactor was set in the vertical position with the protein reservoir on top so that mixing works against gravity – the mixing process is least turbulent in this orientation.

A total of 1292 digitized 'fringe pattern' images were recorded on magnetic tape and also recorded by time-lapse video for real-time analysis *via* an attached PC. The *OPTIMAS* image processing software was configured to define a window in the image and measure the average grey level of the passing fringes within the window. This software can sample the image at many points with a user specified sampling window. In this experiment one window of approximately 0.9×0.2 mm was used, approximately 1.3 mm above the dialysis membrane with its longest length parallel to the membrane as shown in Fig. 2 which also shows an example* of a fringe pattern image.

3. Results and calculations

The motion of fringes, past the sampling window, is indicative of the refractive index change and flow of the chemicals in solution. As each fringe crosses the sampling window a peak is observed in the grey level. The total number of peaks plotted against time are shown in Fig. 3. There is a turning point in the gradient after 40 h. By studying the time-lapse video of the fringe-pattern images it can be seen that the movement of fringes from the bottom of the protein reservoir reverses at this 40 h mark. The intensity of the grey level measured is of essentially sinusoidal form over time with each fringe being regarded as a peak in this sinusoidal varying intensity.

The experiment was stopped after 162 h. Many crystals up to a length of 1.5 mm had grown, all located on the membrane and silicon ring sealing the protein reservoir block to the rest of the reactor. This is because of the siliconization process reducing cohesion to the surface of the reactor walls and the sedimentation effects of gravity.

*Recently we have seen a short note by Kuznetsov, Malkin & McPherson (1995) reporting a Mach-Zehnder interferogram of a single lysozyme crystal.

For a Mach-Zehnder interferometer the change in refractive index between two adjacent black (or white) fringes, caused by concentration gradients within the liquid, can be given (see for example, Steel, 1983) by,

$$\delta n = \frac{\lambda}{d}$$

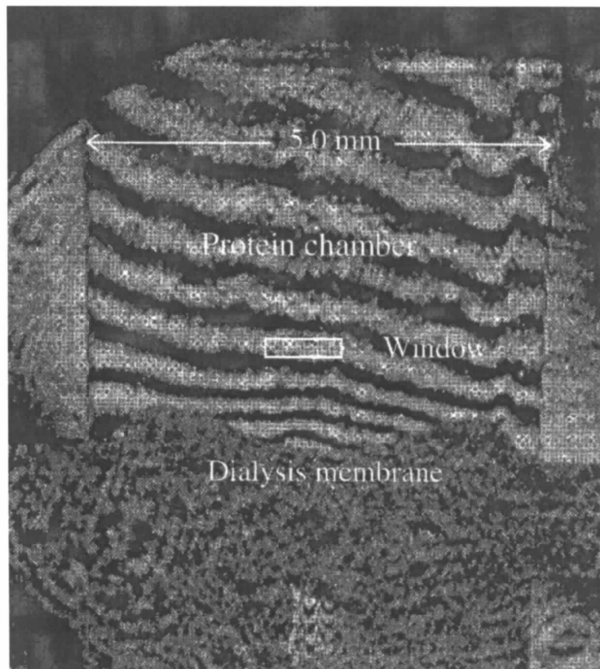


Fig. 2. Example of fringes recorded by the CCD video camera illustrating position and size of the measuring window as a rectangular box. The dialysis membrane boundary is marked with the protein chamber above and salt below.

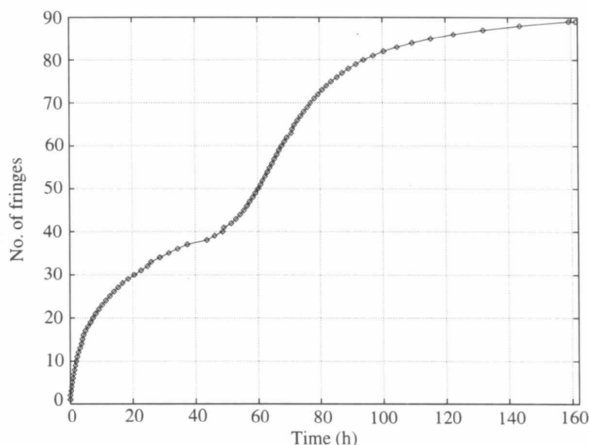


Fig. 3. Cumulative number of fringes passing the sampling window up to any given time. At 40 h the movement of fringes passing through the window stops, and then the direction of fringe movement reverses. In a repeat experiment with identical conditions visual monitoring of crystal growth every 4–8 h showed crystal formation, at around the 40 h mark, thus giving a one-to-one correlation with the fringes behaviour shown in this figure.

In this case λ , the wavelength used in the interferometer, is 780 nm (chosen here because the diode laser is compact and stable) and d , the light path through the protein chamber is 5 mm. Therefore, the change in refractive index between two adjacent fringes, δn , is given by 1.56×10^{-4} .

During the first 40 h of the experiment 37 fringes passed by the sampling window in the direction from the dialysis membrane towards the top of the protein chamber. This corresponds to a refractive index increase in the protein chamber of 5.77×10^{-3} . Thereafter, a total of 52 fringes with motion in the reverse direction were monitored for the remainder of the experiment (122 h) corresponding to a decrease in the refractive index of 8.11×10^{-3} .

The refractive index of water is known at various wavelengths (CRC Handbook of Chemistry and Physics, 1991), Using a Brice-Phoenix differential refractometer with water as the initial reference solution the refractive indices of buffer, salt solution and protein solution were each measured at 436 nm (blue) and 546 nm (green) wavelengths (the operational wavelengths of the available refractometer reference light sources).

By use of the Cauchy formula relating refractive index to wavelength,

$$n_{\lambda} = A + \frac{B}{\lambda^2},$$

where A and B are constants, these refractive index values can be converted to values appropriate for 780 nm, the operational wavelength of the interferometer. At 780 nm the refractive index for 7.34% NaCl solution (7.34 g per 100 ml) is $n_{\text{salt}} = 1.3370$. Likewise, the refractive index of the initial protein solution of 15.8 mg lysozyme per 188 μl buffer is $n_{\text{prot}} = 1.3406$ and for buffer alone is $n_{\text{buff}} = 1.3295$. These points serve then as the starting values for the solutions in the different parts of the reactor prior to the reactor activation.

The changes in refractive index during the crystallization can now be converted into actual changes in salt and/or protein concentration. For every 1 g salt per 100 ml the increment in refractive index can be calculated (Fredericks, Hammonds, Howard & Rosenberger, 1994) as 1.09×10^{-3} . We now make the assumption that the increase in refractive index seen during the first 40 h is entirely as a result of the salt diffusing into the protein chamber. Indeed in a subsequent experiment made with identical conditions and an APCF dialysis reactor monitored by eye every 4–8 h crystal formation appeared to start at about the 40 h point (confirming that our assumption is reasonable). For the increment of 5.77×10^{-3} observed here the salt concentration in the protein chamber reaches 5.29 g per 100 ml or 5.29% ($5.77 \times 10^{-3}/1.09 \times 10^{-3}$).

Once the salt solution has reached equilibrium any change in refractive index will be due to the protein crystallizing out of solution. For every 1 mg lysozyme per 1 ml the refractive index increment can be calculated (Fredericks, Hammonds, Howard & Rosenberger, 1994) as 1.32×10^{-4} . For the increment of -8.11×10^{-3} observed here then we can calculate that, 11.55 mg [($8.11 \times 10^{-3}/1.32 \times 10^{-4}$) \times 0.188] of protein in the reactor has formed into crystals leaving 4.24 mg of protein in solution within the peak to peak measurement (± 0.22 mg).

Each image also provides information on the spatial distribution of refractive index change over time and therefore concentration change. This is shown in Fig. 4. The spatial concentration of salt solution is plotted for images recorded at the 1, 2, 3, 5 and 9 h points.

4. Concluding remarks: main findings, limitations and future work

The changes in concentrations of salt and lysozyme protein in a solution during crystal growth have been monitored as a function of time. The time period for crystal-growth measurements commences at about 40 h after the solutions come into contact across the dialysis membrane as evidenced by the specific change in the concentration gradients in the chamber with time. For the study of other proteins it will be necessary, in some cases, to improve the sensitivity *e.g.* such as for more dilute solutions. The interferometer sensitivity can indeed be improved by use of a shorter wavelength than 780 nm and/or the method of phase shifting (Burning *et al.*, 1974). Phase shifting two-beam interferometry has provided a tenfold increase in sensitivity to concentration changes (Onuma, Tsukamoto & Nakadate, 1993) than does standard two-beam

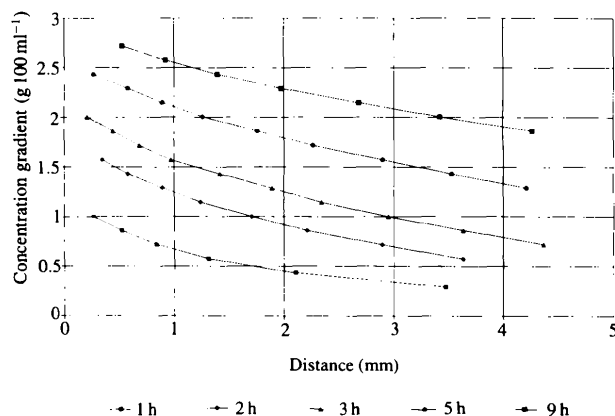


Fig. 4. Plot of concentration of salt solution in the protein chamber at the 1, 2, 3, 5 and 9 h points. Distance 0 mm corresponds to the dialysis membrane and concentration is measured vertically upward from that. Points on the plot correspond to the position of a black fringe.

interferometry. Our analysis has been carried out using peak-to-peak measurements, although the sensitivity can again be improved using profile analysis.

It is obviously fortuitous, in this case here, that the salt solution has reached equilibrium before lysozyme crystallization starts. This may not generally be the case. Deconvoluting the separate processes of diffusion and crystallization would then have to use other information, for example mathematically modelling the salt diffusion process (Wagner & Linhardt, 1991) and using that to determine the protein dependent refractive index change. Alternatively, use of a coloured protein and colour CCD or UV CCD monitoring could be made to evaluate the quantity of protein leaving solution and crystallizing at any given time. Nevertheless, in our experiments here, the turning point in the lysozyme crystallization cumulative fringe curve (Fig. 3) produces a clear indication of the point where crystallization starts (*i.e.* after 40 h). This result was subsequently correlated with simple 'by eye' monitoring of the crystal growth process in a repeat experiment.

In essence, interferometry is useful to give insight into the diffusion kinetics during crystal growth, including the chance, in the future, to monitor the alterations in the fringe behaviour in microgravity compared with earth, and thereby gain further insight into the protein crystal growth process.

R. Bosch and J. Stapelmann from Dornier GmbH are acknowledged for their help and assistance (and providing access to the engineering model of the interferometer) during the experiment at Dornier. R.

Pinfield and S. Cooper are acknowledged for their help at the University of Manchester in the use of the differential refractometer and the spectrophotometer, respectively.

References

- Bosch, R., Lautenschlager, P., Potthast, L. & Stapelmann, J. (1992). *J. Cryst. Growth*, **122**, 310-316.
- Burning, J. H., Herriot, D. R., Gallagher, J. E., Rosenfeld, D. P., White, A. D. & Brangaccio, D. J. (1974). *Appl. Opt.* **13**, 2693.
- CRC Handbook of Chemistry and Physics (1991). 72nd Edition, pp. 10-289. Boca Raton, Florida: CRC Press.
- Fredericks, W. J., Hammonds, M. C., Howard, S. B. & Rosenberger, F. (1994). *J. Cryst. Growth*, **141**, 183-192.
- Kuznetsov, Y. G., Malkin, A. J. & McPherson, A. (1995). *Hampton Res. News*, **5**(2), 27.
- Helliwell, J. R. (1988). *J. Cryst. Growth*, **90**, 259-272.
- Helliwell, J. R., Snell, E. & Weisgerber, S. (1996). *Proceedings of the Berlin Microgravity Conference 1995*. Berlin: Springer Verlag. In the press.
- Onuma, K., Tsukamoto, K. & Nakadate, S. (1993). *J. Cryst. Growth*, **129**, 706-718.
- Shlichta, P. J. (1986). *J. Cryst. Growth*, **76**, 656-662.
- Snell, E., Weisgerber, S., Helliwell, J. R., Weckert, E., Hölzer, K. & Schroer, K. (1995). *Acta Cryst.* **D51**, 1099-1102.
- Snyder, R. S., Fuhrmann, K. & Walter, H. U. (1991). *J. Cryst. Growth*, **110**, 333-338.
- Steel, W. H. (1983). *Interferometry*. Cambridge University Press.
- Wagner, G. & Linhardt, R. (1991). *J. Cryst. Growth*, **110**, 114-118.